

# FORCE/POSITION CONTROL FOR AN EXCAVATOR WITH CONTOUR CONTROL COMPENSATION

Niraj Reginald<sup>1</sup>, Jaho Seo<sup>1</sup>

<sup>1</sup>*Department of Mechanical Engineering, University of Ontario Institute of Technology, Oshawa, ON, Canada.*

*E-mail: nirajreginald@gmail.com; jaho.seo@uoit.ca*

---

## ABSTRACT

The main objective of this paper is to provide an integrative control strategy for an autonomous operation of electro-hydraulic excavators that can simultaneously deal with position, contour and force controls required for ground contact tasks. For system modeling, kinematic and dynamic analyses of an excavator manipulator was conducted and a hydraulic system including valves and cylinders were modeled. As a part of control strategy, a position controller using a nonlinear PI technique was designed to control the cylinder's stroke and thus bucket tip by considering hydraulic system's uncertainties. For the force control that is required to maintain the vertical position of bucket tip (leveling) despite unexpected external ground loads, an impedance controller based on the time delayed joint space control scheme was designed. To generate an optimal trajectory of the bucket tip, a contour control compensation was introduced. Simulation results show that the designed control scheme provides good force and position tracking performance along with contour control compensation in terms of accuracy and response time for a leveling task.

**Keywords:** excavator; impedance control; contour control, position control

---

## COMMANDE DE FORCE ET DE POSITION POUR UNE PELLE AVEC COMPENSATION DE COMMANDE DE CONTOUR

### RÉSUMÉ

L'objectif principal de cet article est de fournir une stratégie de contrôle intégrative pour un fonctionnement autonome des pelles électro-hydrauliques qui peut gérer simultanément les contrôles de position, de contour et de force pour les tâches de contact au sol. Pour la modélisation du système, des analyses cinématiques et dynamiques d'un manipulateur de pelle ont été réalisées et un système hydraulique comprenant des vannes et des cylindres a été modélisé. Dans le cadre de la stratégie de contrôle, un contrôleur de position utilisant la technique PI non linéaire a été conçu pour contrôler la course du cylindre et donc la pointe du godet en tenant compte des incertitudes du système hydraulique. Pour le contrôle de la force nécessaire au maintien de la position verticale de la pointe du godet (nivellement) malgré des charges au sol externes inattendues, un contrôleur d'impédance basé sur le schéma de contrôle de l'espace du joint retardé (temporization) a été conçu. Pour générer une trajectoire optimale de la pointe du godet, une compensation de contrôle de contour a été introduite. Les résultats de la simulation montrent que le contrôleur conçu fournit les bonnes performances de suivi de la force et de la position ainsi que la compensation de la commande de contour en termes de précision et de temps de réponse pour une tâche de nivellement.

**Mots-clés:** pelle; commande d'impédance; commande de contour; commande de position

# 1 INTRODUCTION

Excavators are earthmoving machines, which are used for tasks where contact with the ground is involved. The main tasks for excavators include digging, carrying loads, dumping loads, trenching and ground levelling [1]. In conventional excavators, operators mostly control four links (manipulators) using joysticks and therefore efficiency and accuracy of works carried out by excavators could be improved through automation and autonomization using robotics techniques. There have been technical advances in automation excavation to enhance productivity and safety, and to reduce operational costs and dependency of skilled workers.

For the automated excavation, previous studies have proposed methodologies to track a desired reference position using various control techniques such as fuzzy logic [2], neural networks [2–4], PID controllers with optimization techniques [5,6], nonlinear PI controllers [7], etc.

Contour control is one of crucial components for automation and autonomization of excavators since generation and tracking of an optimized contour trajectory enable more efficient and safer ground tasks that require sophisticated and coordinated control of the boom, arm, and bucket links.

Contour control targets to reduce the tracking error between actual position and its reference, and the contour error that is defined as the smallest possible distance from current actual position to the reference trajectory. A few researches have been carried out to circumvent the contour error in the area of excavation [7,8].

The most challenging part of tracking control for autonomous excavation is force control by considering that resistive ground force (external load) prevents an accurate tracking of trajectory. As a remedy for this problem, an impedance control strategy could be more suitable to deal with excavator dynamics rather than position control since it is able to provide a unified approach for the bucket tip control in both contact and non-contact space. To deal with this issue, there have been several studies in force control for excavators using impedance control technique [1, 9–11] but relatively little attention has been received in this area compared to the position tracking control.

Modelling of the dynamics of manipulators in excavators is difficult due to uncertain behaviors arising from hydraulic and mechanical components (e.g. actuation friction, hysteresis and other unmolded dynamics). Therefore, an appropriate control strategy to take the uncertain dynamics into consideration is a prerequisite for autonomous excavation. Since the excavator has links and joints and therefore can be considered as a robot manipulator system. Some existent modeling methodologies in robotic engineering can be applicable to tackle uncertain dynamics in excavator dynamic models. For an example, a time-delayed joint space control [12–15] have been used as a technique to compensate for uncertainties in robot dynamics.

Position, contour and force controls are mutually associated factors influencing successful autonomous operation of excavators. Although previous studies have addressed these factors, most past studies have been limited to investigating individual aspects (not all simultaneously). In this study, an integrated control strategy is proposed by considering all the perspectives of position, contour, and force controls of excavators under uncertain dynamics. The rest of this article is organized as follows. In section 2, a methodology for modeling the excavator dynamics is described. Section 3 describes the algorithms of the designed position, contour and force impedance controllers. Section 4 presents simulation results, and concluding remarks are provided in section 5.

## 2 MODELLING OF EXCAVATOR

The system model of the excavator developed in this study consists of three components that are kinematics, dynamics and hydraulic models. Mathematical models for each component will be explained in the following sections.

### 2.1 Kinematics modelling of excavator

The coordinate systems of  $O_1 \rightarrow [X_1, Y_1, Z_1]$ ,  $O_2 \rightarrow [X_2, Y_2, Z_2]$ ,  $O_3 \rightarrow [X_3, Y_3, Z_3]$ ,  $O_4 \rightarrow [X_4, Y_4, Z_4]$  as shown in Fig. 1 are assigned according to the Denavit-Hartenberg procedure as described in [16].

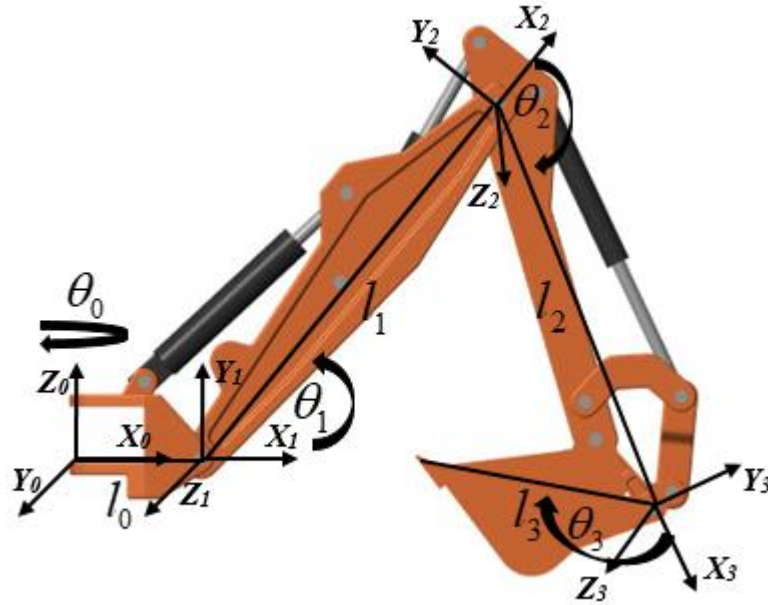


Fig. 1. D-H coordinate system for excavator system

The excavator bucket tip position can then be expressed as given in Eq. (1)

$$\begin{cases} x = \cos(\theta_0)[l_3 \cos(\theta_1 + \theta_2 + \theta_3) + l_2 \cos(\theta_1 + \theta_2) + l_1 \cos(\theta_1)] \\ y = \sin(\theta_0)[l_3 \sin(\theta_1 + \theta_2 + \theta_3) + l_2 \sin(\theta_1 + \theta_2) + l_1 \sin(\theta_1)] \\ z = l_3 \sin(\theta_1 + \theta_2 + \theta_3) + l_2 \sin(\theta_1 + \theta_2) + l_1 \sin(\theta_1) \\ \gamma = \theta_1 + \theta_2 + \theta_3 \end{cases} \quad (1)$$

Where  $\gamma$  is the orientation of the excavator end effector. Similarly if  $[x y z \gamma]^T$  is given, we can obtain  $\theta(t) = [\theta_0 \theta_1 \theta_2 \theta_3]$  using inverse kinematics. Since most excavators do not use the swing motion when performing ground contact tasks,  $\theta_0$  is assumed to be zero, and then Eq. (1) can be simplified as

$$\begin{cases} x = l_3 \cos(\theta_1 + \theta_2 + \theta_3) + l_2 \cos(\theta_1 + \theta_2) + l_1 \cos(\theta_1) \\ z = l_3 \sin(\theta_1 + \theta_2 + \theta_3) + l_2 \sin(\theta_1 + \theta_2) + l_1 \sin(\theta_1) \\ \gamma = \theta_1 + \theta_2 + \theta_3 \end{cases} \quad (2)$$

## 2.2 Dynamics model of excavator

The well-known form of dynamic equation for the motion of excavator manipulator has been presented in [11,17].

$$D(\theta)\ddot{\theta} + H(\theta, \dot{\theta}) = \tau(\theta) - \tau_e(\theta) \quad (3)$$

where  $D(\theta)$  is an  $n \times n$  inertial matrix,  $H(\theta, \dot{\theta})$  is an  $n \times 1$  combined Coriolis, centrifugal and gravity vector.  $\tau(\theta)$  is the  $n \times 1$  joint torque vector generated by the manipulator, and  $\tau_e(\theta)$  is the external joint torque applied to the manipulator by the environment. Time delayed control method was incorporated in

previous work [18] to mitigate the uncertainties of a robot manipulator dynamics. Considering Eq. (3), we can estimate  $H(\theta, \dot{\theta})$  in time domain as follows if the sample time is short enough.

$$H(t) \approx H(t - \delta) = \tau(t - \delta) - \tau_e(t - \delta) - \tilde{D}\dot{\theta}(t - \delta) \quad (4)$$

Where  $\tilde{D}$  is an  $n \times n$  diagonal estimated matrix of  $D(\theta)$  and  $\delta$  is the sample time. Assuming that the inertia of the excavator does not change suddenly, we can incorporate this method to estimate the unmodeled dynamic components.

### 2.3 Hydraulic Valve and Cylinder Model of an excavator

As shown in Fig. 2, the electro-hydraulic valve system for a robotic excavator works in a way that a desired control voltage for target cylinder position is generated. This voltage is converted to current using a servo valve current amplifier that controls the servo valve spool displacement by opening and closing thereby controlling the flow through the valve. The current amplification stage of the system can be expressed as a pure proportional stage given in Eq. (5).

$$i_v = K_a u \quad (5)$$

where  $i_v$  is the amplified output current to the valve,  $K_a$  is the proportional current amplifier coefficient and  $u$  is the input control voltage generated by the controller.

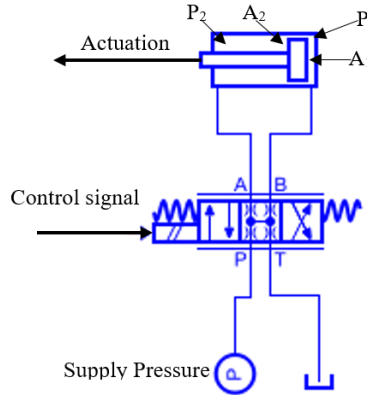


Fig. 2. Hydraulic Valve and Cylinder Model

A linearized load flow equation for a servo valve can be expressed as below using a Taylor series linearization [19] given that the valve is assembled with ideal zero lapping, zero opening, and matched symmetrically [5].

$$Q_{Lv} = K_q x_v - K_c P_L \quad (6)$$

where  $Q_{Lv}$  is the flow across the servo valve,  $K_q$  is the valve flow coefficient,  $K_c$  is the valve flow-pressure gain,  $x_v$  is the spool servo valve displacement and  $P_L$  is the load pressure given as  $P_L = P_1 - P_2$  where  $P_1$  is cylinder head side pressure, and  $P_2$  is cylinder rod side pressure. The flow continuity equation for cylinders can be expressed as

$$Q_{LP} = C_{tp} P_L + A_p \dot{x}_p + \frac{V_e}{4\beta_e} \dot{P}_L + Q_{lad} \quad (7)$$

where  $Q_{LP}$  is the flow continuity of cylinder,  $A_p$  is the equivalent piston area, and  $x_p$  is the piston position of the cylinder.  $C_{tp}$  is the total leakage coefficient,  $V_t$  is total cylinder volume,  $V_e$  is the equivalent

cylinder volume,  $Q_{lad}$  is any other additional leakage flow, and  $\beta_e$  is the effective bulk modulus of the hydraulic oil, and

$$\left. \begin{aligned} A_p &= (A_1 + A_2) / 2 \\ C_{ip} &= \{C_{ip} \text{ (internal leakage coefficient)} + C_{ep} \text{ (external leakage coefficient)}\} / 2 \\ V_t &= A_1 L \\ V_e &= \frac{2V_t \left( \eta^2 + \frac{V_1}{V_t} (1 - \eta^2) \right)}{1 + \eta^2} \text{ where } \eta = \frac{A_2}{A_1} \end{aligned} \right\} \quad (8)$$

where  $A_1$  is the piston head side diameter,  $A_2$  is the cylinder rod side diameter,  $V_t$  is the total cylinder volume, and  $V_e$  is the equivalent cylinder volume.

The dynamic model of the cylinder is described using the load force of inertia, elastic force, viscous friction, and external forces [20]. The force equation for the cylinder can be given as

$$A_p P_L = M_t \frac{d^2 x_p}{dt^2} + B_p \frac{dx_p}{dt} + F_L + K_s x_p \quad (9)$$

where  $M_t$  is the gross mass of piston and load,  $B_p$  is the viscous damping coefficient,  $F_L$  is the external disturbance, and  $K_s$  is the spring constant.

The dynamic model for the proportional directional valve spool can be given as

$$\frac{d^2 x_v}{dt^2} + 2\delta_v \omega_v \frac{dx_v}{dt} + \omega_v^2 x_v = K_a K_v \omega_v^2 u \quad (10)$$

where  $\delta_v$  is the valve damping ratio,  $\omega_v$  is the valve natural frequency,  $K_a$  is the proportional amplification coefficient,  $K_v$  is the gain of spool displacement-current (m/A),  $u$  is the valve control signal, and  $x_v$  is valve spool position. Using Eqs. (6) and (7) and taking Laplace transformations, we can express  $P_L$  as

$$P_L = \frac{K_q X_v - A_p S X_p - Q_{lad}}{K_c + C_{ip} + \frac{V_e}{4\beta_e} S} \quad (11)$$

Substituting  $P_L$  to the Laplace transformed Eq. (9), the transfer function  $Z_I(S)$  between the valve position and cylinder position can be obtained.

$$Z_I(S) = \frac{X_p}{X_v} = \frac{\frac{K_q}{A_p}}{S \left( \frac{S^2}{\omega_h^2} + \frac{2\zeta_h S}{\omega_h} + 1 \right)} \quad (12)$$

where  $\omega_h = A_p \sqrt{\frac{4\beta_e}{V_e M_t}}$  and  $\zeta_h = \frac{K_{ce}}{A_p} \sqrt{\frac{\beta_e M_t}{V_e}}$ .

Taking Laplace transformations for Eq. (10), we can obtain the transfer function between the valve control signal and valve position.

$$Z_2(S) = \frac{X_v}{U} = \frac{K_a K_v}{\frac{S^2}{\omega_v^2} + \frac{2\delta_v S}{\omega_v} + 1} \quad (13)$$

Finally, the transfer function between cylinder position and the control signal  $G(s)$  can be obtained as

$$G(S) = \frac{X_p}{U} = Z_1(S).Z_2(S) \quad (14)$$

### 3 CONTROL TECHNIQUES FOR EXCAVATOR

The following Fig. 3 shows a schematic of the designed controller that integrates the position, contour and force controls.

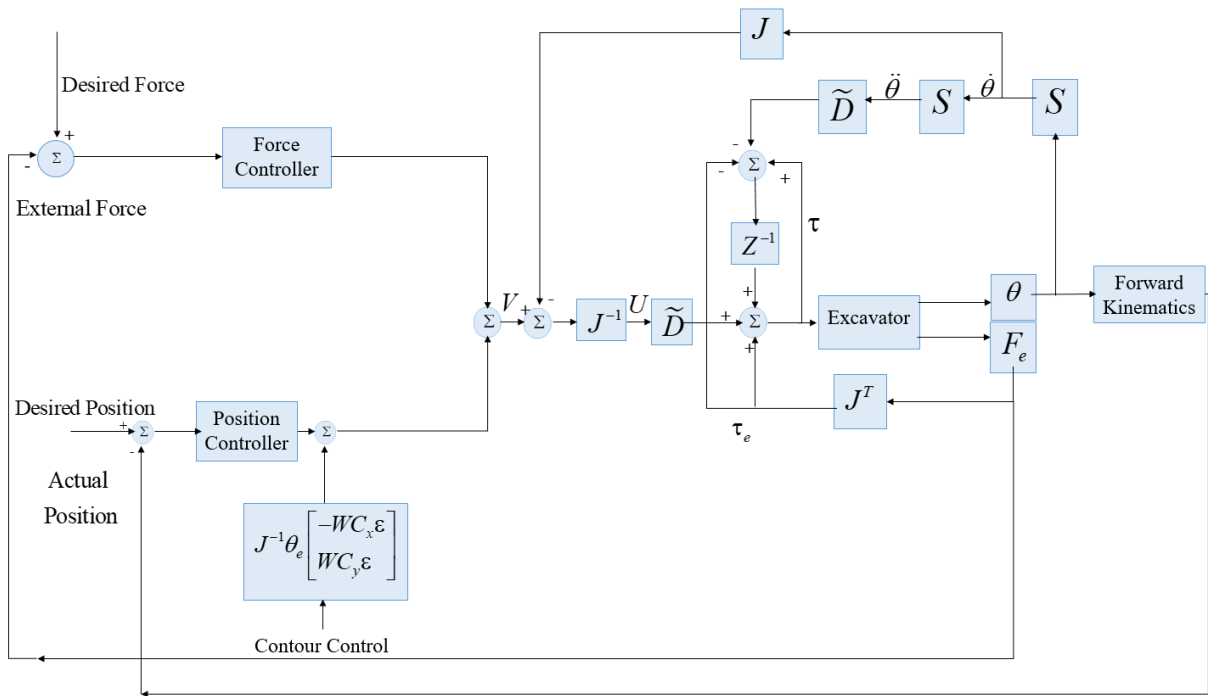


Fig. 3. Control Diagram

#### 3.1 Cylinder Position control

Hydraulic cylinder position control can be challenging due to its inherent dynamic uncertainties such as valve dead zone, friction, leakages and other uncertainties. Also, when the bucket tip is in contact with the environment, the effective forces can vary according to even small deviations in position. Due to this reason, it is required to apply a control strategy that can quickly and accurately adapt to small deviations in reference trajectory. A nonlinear PI control method was used to address and compensate for the uncertainties mentioned above for an industrial hydraulic manipulator [21] and an excavator system [7]. Eq. (15) shows the integral of the applied nonlinear PI controller.

$$I_t = (I_{t-\delta t} + e\delta t + K_a \ddot{\theta}_d \delta t) \frac{a}{a + \dot{e}^2} \quad (15)$$

where  $e$  is the error,  $\delta t$  is the sampling time,  $\ddot{\theta}_d$  is the target angular acceleration,  $K_a$  and  $a$  are constants.

### 3.2 Contour control

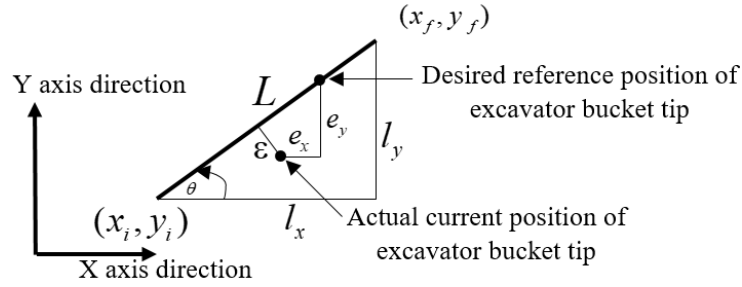


Fig. 4. Contour error and Tracking error for a reference path

Figure 4 describes contour and tracking errors for a reference trajectory. The tracking error (either  $e_x$  in  $x$  axis or  $e_y$  in  $y$  axis) is the direct vector difference between the desired reference position and current position of the bucket tip.  $\varepsilon$  is the contour error, known as the shortest distance to the desired reference trajectory from the actual current position. The contour error can be calculated using Fig. 4 in terms of tracking errors, and be decomposed into  $x$  and  $y$  axes as shown below:

$$e_c = \begin{bmatrix} e_{cx} \\ e_{cy} \end{bmatrix} = \begin{bmatrix} C_x \varepsilon \\ C_y \varepsilon \end{bmatrix} \quad (16)$$

where  $C_x = \sin \theta = \frac{l_y}{L}$  and  $C_y = \cos \theta = \frac{l_x}{L}$ .

The final goal of contour control is to reduce the contour error  $\varepsilon$  along with the tracking error. The contour error described as  $e_c$  in Cartesian space can be converted to joint space using the Jacobian matrix given that the errors are adequately small.

$$\theta_e = J^{-1} e_c \quad (17)$$

Since the bucket link length is much smaller than that of the boom and arm link, a major deviation to the contour error is caused by the arm and boom. In order to reduce the contour error as given in Fig. 4, it should be subtracted from the current position in  $x$  direction, and simultaneously be added to the current position in  $y$  direction. Considering the contour compensation is added to the position control signal for the arm and boom, the compensation control signal can be denoted as

$$U_c = \begin{bmatrix} -U_{cx} \\ U_{cy} \end{bmatrix} = J^{-1} \theta_e \begin{bmatrix} -w_1 C_x \varepsilon \\ w_2 C_y \varepsilon \end{bmatrix} \quad (18)$$

where  $w_1$  and  $w_2$  are tuning parameters that can be used to optimize the sensitivity of the compensation control signal.

### 3.3 Force impedance control

The dynamic relationship between the excavator and the environment can be considered as an impedance function as follows.

$$M\ddot{E} + B\dot{E} + KE = F_E \quad (19)$$

where  $E$  is the error between the desired reference location  $X_r$  and actual current location  $X$ ;  $F_E$  is the external force from the environment;  $M$ ,  $B$ , and  $K$  as the impedance gains. In order to integrate force tracking capabilities to Eq. (19), the following equation incorporates the desired force,  $F_d$  and environment position  $X_e$  [15], which yields the force tracking capability for the impedance function.

$$M\ddot{\varepsilon} + B(\dot{\varepsilon} + w) = f_e - f_d \quad (20)$$

where  $\varepsilon = X_e - X$  and  $w$  is the adaptive law given as  $w(t) = w(t - \delta) + \eta \frac{f_d(t - \delta) - f_e(t - \delta)}{b}$ .  $\delta$  is the sample time,  $\eta$  is the adaptive gain to tune, and  $b$  is an impedance gain. As shown in Fig. 3,  $V$  is defined as

$$v = \begin{cases} \frac{1}{M} (B(\dot{\varepsilon} + w) + F_d - F_e) & \text{for force control direction} \\ \ddot{X}_d + K_D \dot{e} + K_P e & \text{for position control direction} \end{cases} \quad (21)$$

where  $K_D$  and  $K_P$  are controller gains. The torque  $\tau$  and control law  $U$  is given as in Eqs. (22) and (23).

$$\tau(t) = \tau(t - \delta) = \tilde{D}U + H(t - \delta) + \tau_e(t - \delta) \quad (22)$$

$$U = \ddot{\theta} = J^{-1}(V - \dot{J}\dot{\theta}) \quad (23)$$

## 4 SIMULATION RESULTS

The ground levelling task was considered as a scenario to evaluate the performance of the designed controller through simulations. For the levelling task, the bucket tip of an excavator was asked to follow a linear contour profile from (6m, 1.5m) to (4.5m, 0m). Table 1 shows specifications of modeled cylinders and link lengths that were used for the simulations.

Table 1. Main Physical parameters

	Boom (mm)	Arm (mm)	Bucket (mm)
Link Lengths	4600	2525	1622
Cylinder Stroke	950	1130	875
Cylinder Head Diameter	105	116	100
Cylinder Rod Diameter	70	80	70

The contact environment was assumed to have a time varying stiffness and damping in  $y$  axis, and a fixed stiffness and damping along the  $x$  axis in order to validate the designed controller's performance in varying conditions. The force exerted by the environment  $F_e$  can be modelled as [15]:

$$F_e = K_e (X - X_e) + B_e (\dot{X} - \dot{X}_e) \quad (24)$$

The stiffness element of  $K_e$  in  $x$  axis ( $k_{ex}$ ) was set to 1000 N/m and damping coefficient element of  $B_e$  in  $x$  axis direction ( $b_{ex}$ ) was set to 100 Ns/m. The stiffness element of  $K_e$  in  $y$  axis ( $k_{ey}$ ) direction and damping coefficient element of  $B_e$  in  $y$  axis direction ( $b_{ey}$ ) were set to  $1000 + 1000\sin(\pi t / 6)$  N/m and  $100 + 100\sin(\pi t / 6)$  Ns/m, respectively. The second requirement for the leveling task is to keep a force tracking of  $F_d = [-5N, -10N]^T$  in  $x$  and  $y$  axis directions. MATLAB®/Simulink was used to model and simulate the system, and a sampling time of 0.004 was set with a simulation time of 10 sec.  $\eta = 0.2$  was used as the force tracking adaptive gain for the simulation. Figs. 5 and 6 present that the designed force controllers show good force tracking performance in  $y$  and  $x$  axis, respectively.

Figs. 7 and 8 present the position tracking performance in  $y$  and  $x$  axis. One can note that the bucket tip can successfully trace the reference position in terms of accuracy and response time, and the addition of the contour compensation contributes to reducing tracking errors and response time by generating an optimized trajectory.

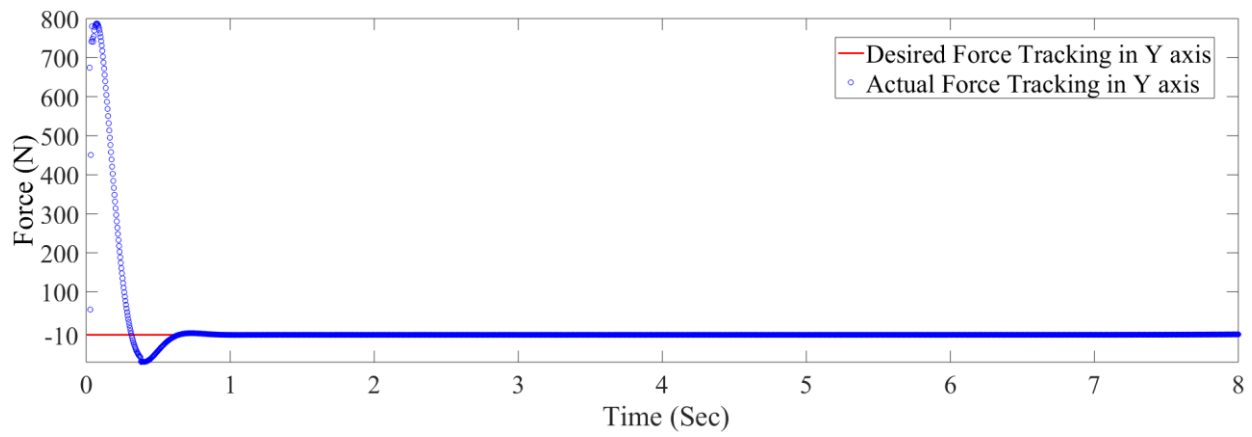


Fig. 5. Force Tracking in Y axis

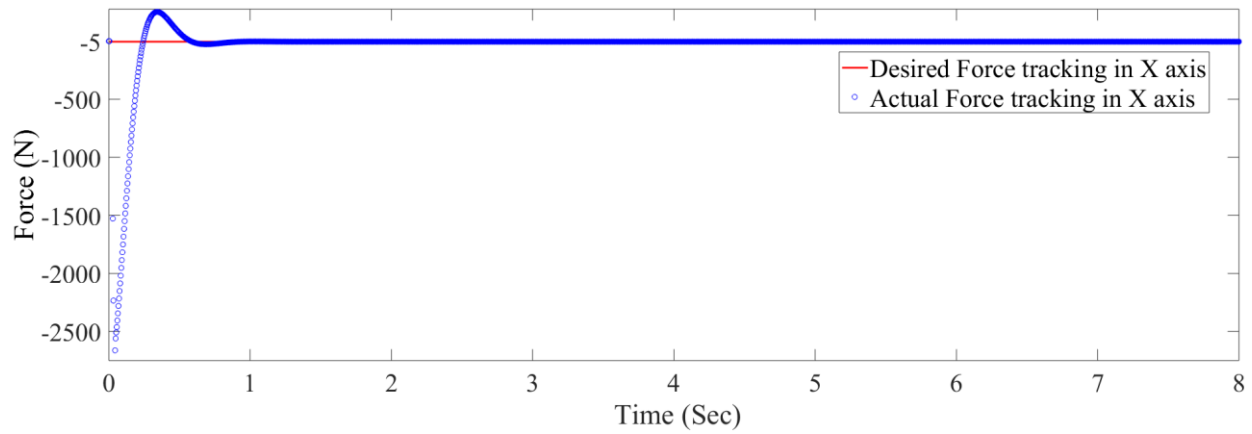


Fig. 6. Force Tracking in X axis

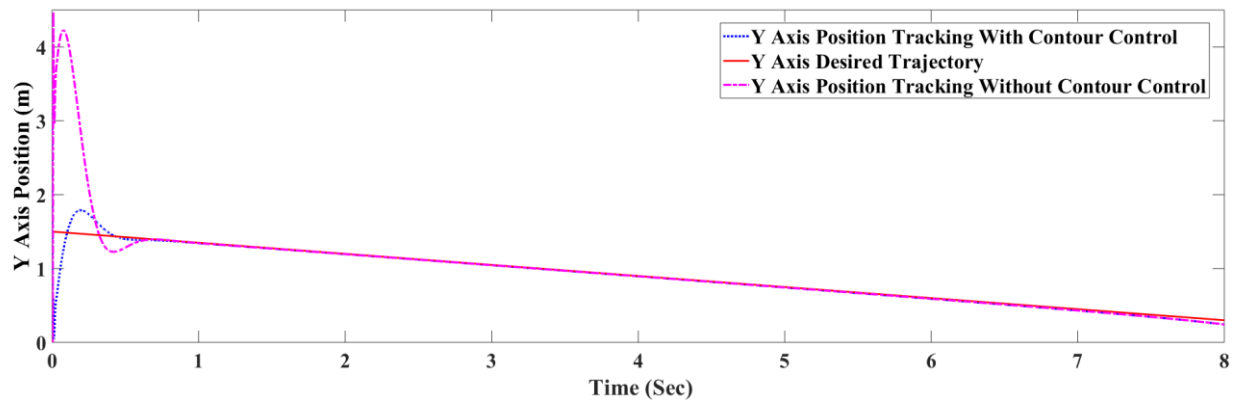


Fig. 7. Y axis Position Tracking Results

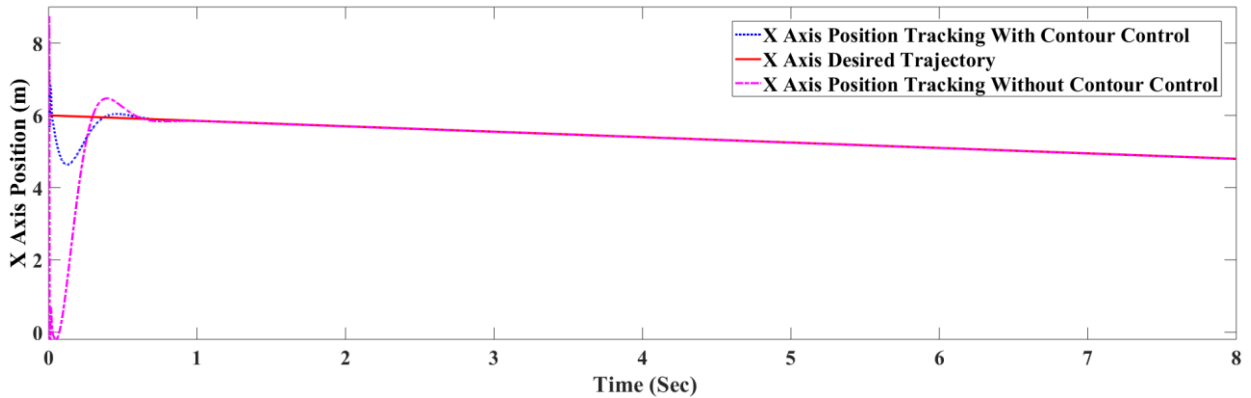


Fig. 8. X Axis Position Tracking Results

Simulation results in Fig. 9 and 10 confirm that the contour compensation improves the tracking performance by decreasing the RMS values (Root Mean Square) of tracking errors. Compensation factors  $W_1 = 0.2$  and  $W_2 = 0.3$  were used for the simulations in Figs. 7-10.

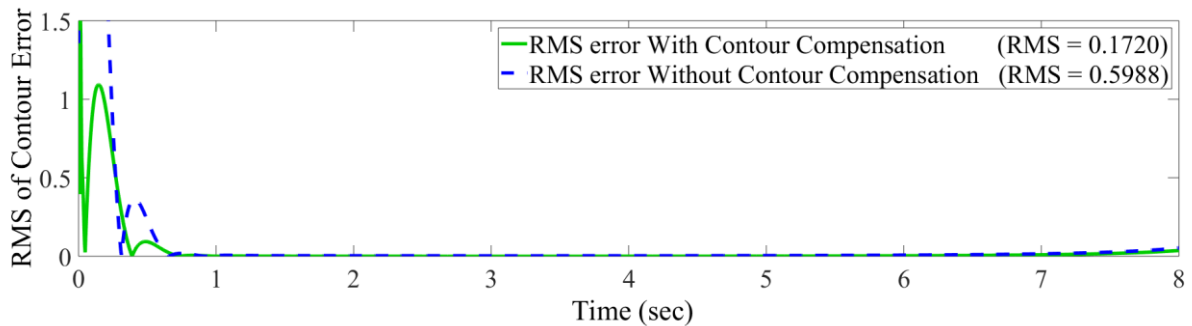


Fig. 9. Root Mean Square Error of Contour Error

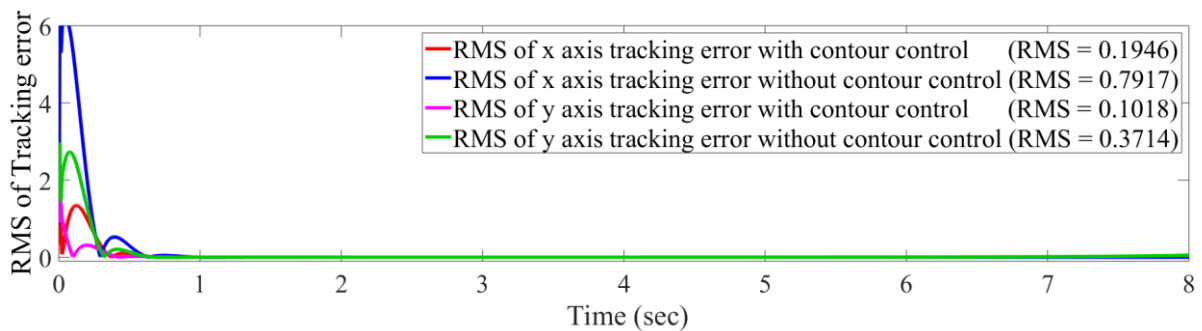


Fig. 10. Root Mean Square Error of Tracking Error

Finally, Figs. 11 and 12 show that the designed non-linear PI controller for stroke tracking of arm and boom cylinders is relatively superior to a normal linear PI control in terms of faster response time (i.e., decreased settling time), and thus provides a better control solution to deal with uncertain dynamics of hydraulic excavator systems.

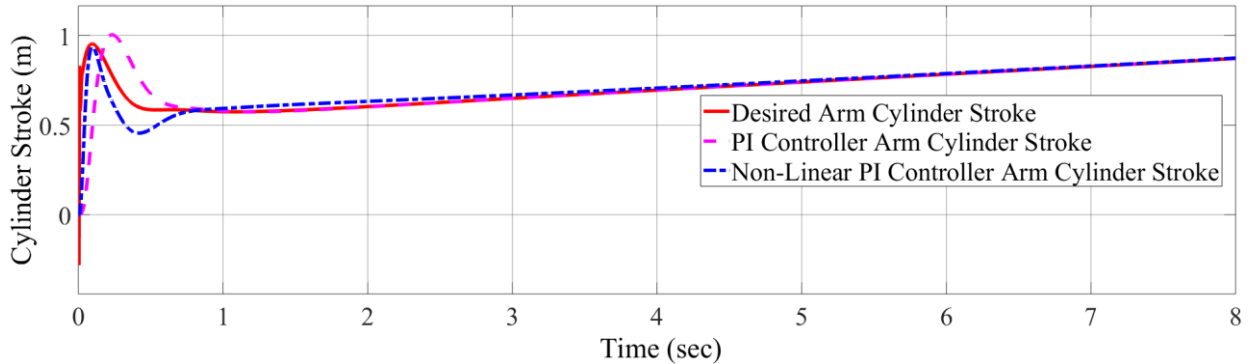


Fig. 11. Arm Cylinder Stroke Tracking

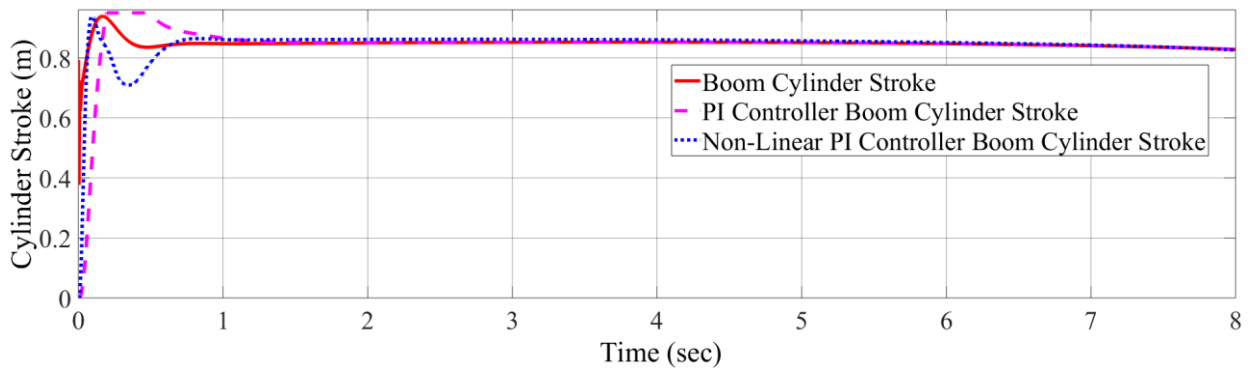


Fig. 12. Boom Cylinder Stroke Tracking

## 5 CONCLUSIONS

This study presented a full tracking control strategy for autonomous operations of hydraulic excavators that considers position, force, and contour control, simultaneously. Simulation results show that for the considered ground levelling task, the proposed impedance control algorithm provided good force tracking results despite dynamic uncertainties of the excavator system. From the results, it can be also seen that the designed cylinder position controller consisting of non-linear PI controller and contour error compensation provides an optimized solution in reducing both position and contour errors.

As a future work, an experimental validation on the performance of the designed control algorithms using a test bench (a mini hydraulic excavator) is considered. An estimation of resistive ground forces during the ground contact work under various conditions (e.g., digging angles, width/thickness of the cutting slice of soil) with the aid of machine learning could be extensive work.

## REFERENCES

1. S. E. Salcudean, S. Tafazoli, P. D. Lawrence, and I. Chau, "Impedance control of a teleoperated mini excavator," *1997 8th International Conference on Advanced Robotics. Proceedings. ICAR'97*, Vol. 10, No. 3, pp. 355–367, 1997.
2. D. Le Hanh, K. K. Ahn, N. B. Kha, and W. K. Jo, "Trajectory control of electro-hydraulic excavator using fuzzy self tuning algorithm with neural network," *Journal of Mechanical Science and Technology*, Vol. 23, No. 1, pp. 149–160, 2009.
3. J. Park, D. Cho, S. Kim, Y. B. Kim, P. Y. Kim, and H. J. Kim, "Utilizing online learning based on echo-state networks for the control of a hydraulic excavator," *Mechatronics*, Vol. 24, No. 8, pp. 986–1000, Dec. 2014.

4. D. Zhenmian, Y. Zhengmao, Z. Hui, B. Hua, X. Yuanli, and J. Xianguo, "The study of trajectory automatic control based on RBF neural network PID control," in *2015 International Conference on Fluid Power and Mechatronics (FPM)*, 2015, pp. 1234–1238.
5. Y. Ye, C. B. Yin, Y. Gong, and J. jing Zhou, "Position control of nonlinear hydraulic system using an improved PSO based PID controller," *Mechanical Systems and Signal Processing*, Vol. 83, pp. 241–259, 2017.
6. H. Feng *et al.*, "Robotic excavator trajectory control using an improved GA based PID controller," *Mechanical Systems and Signal Processing*, Vol. 105, pp. 153–168, 2018.
7. D. Wang, L. Zheng, H. Yu, W. Zhou, and L. Shao, "Robotic excavator motion control using a nonlinear proportional-integral controller and cross-coupled pre-compensation," *Automation in Construction*, Vol. 64, pp. 1–6, 2016.
8. C. S. Lee, J. Bae, and D. Hong, "Contour control for leveling work with robotic excavator," *International Journal of Precision Engineering and Manufacturing*, Vol. 14, no. 12, pp. 2055–2060, 2013.
9. Q. H. Nguyen, Q. P. Ha, D. C. Rye, and H. F. Durrant-Whyte, "Force/position tracking for electrohydraulic systems of a robotic excavator," in *Proceedings of the 39th IEEE Conference on Decision and Control (Cat. No.00CH37187)*, 2006, Vol. 5, pp. 5224–5229.
10. S. Tafazoli, S. E. Salcudean, K. Hashtrudi-Zaad, and P. D. Lawrence, "Impedance control of a teleoperated excavator," *IEEE Transactions on Control Systems Technology*, Vol. 10, No. 3, pp. 355–367, 2002.
11. Q. P. Ha, Q. H. Nguyen, D. C. Rye, and H. F. Durrant-Whyte, "Impedance control of a hydraulically actuated robotic excavator," *Automation in construction*, Vol. 9, No. 5, pp. 421–435, 2000.
12. T. C. Hsia and L. S. Gao, "Robot manipulator control using decentralized linear time-invariant time-delayed joint controllers," in *Proceedings., IEEE International Conference on Robotics and Automation*, 1990, pp. 2070–2075.
13. S. Jung, T. C. Hsia, and R. G. Bonitz, "Force Tracking Impedance Control for Robot Manipulators with an Unknown Environment: Theory, Simulation, and Experiment," *The International Journal of Robotics Research*, Vol. 20, No. 9, pp. 765–774, Sep. 2001.
14. S. Jung, T. C. Hsia, and R. G. Bonitz, "Force Tracking Impedance Control of Robot Manipulators Under Unknown Environment," *IEEE Transactions on Control Systems Technology*, Vol. 12, No. 3, pp. 474–483, May 2004.
15. S. Jung and T. C. Hsia, "Force Tracking Impedance Control of Robot Manipulators for Environment with Damping," in *IECON 2007 - 33rd Annual Conference of the IEEE Industrial Electronics Society*, 2007, No. 1, pp. 2742–2747.
16. B. Zhang, S. Wang, Y. Liu, and H. Yang, "Research on Trajectory Planning and Autodig of Hydraulic Excavator," *Mathematical Problems in Engineering*, Vol. 2017, pp. 1–10, 2017.
17. A. J. Koivo, M. C. Ramos, and M. Thoma, "Dynamic model for excavators (and backhoes)," *IFAC Proceedings Volumes*, Vol. 27, No. 14, pp. 763–768, 1994.
18. T. A. Lasky and T. C. Hsia, "On force-tracking impedance control of robot manipulators," in *Proceedings. 1991 IEEE International Conference on Robotics and Automation*, 1991, no. April, pp. 274–280.
19. T. Knohl and H. Unbehauen, "Adaptive position control of electrohydraulic servo systems using ANN," *Mechatronics*, Vol. 10, No. 1–2, pp. 127–143, Feb. 2000.
20. H. Han, Y. Liu, L. Ma, and Z. Liu, "Analyze the characteristics of electro-hydraulic servo system's position-pressure master-slave control Advances," *Advances in Mechanical Engineering*, Vol. 10, No. 6, pp. 1–9, 2018.
21. N. Sepehri, a. a. Khayyat, and B. Heinrichs, "Development of a nonlinear PI controller for accurate positioning of an industrial hydraulic manipulator," *Mechatronics*, Vol. 7, No. 8, pp. 683–700, 1997.